Composites: Part A 150 (2021) 106628

Contents lists available at ScienceDirect

Composites Part A

journal homepage: www.elsevier.com/locate/compositesa

Modulating impact resistance of flax epoxy composites with thermoplastic interfacial toughening

F. Javanshour [a,*], A. Prapavesis [b], T. Pärnänen [a], O. Orell [a], M.C. Lessa Belone [a], R.K. Layek [c], M. Kanerva [a], P. Kallio [d], A.W. Van Vuure [b], E. Sarlin [a]

[a] Department of Materials Science and Environmental Engineering, Tampere University, Tampere, Finland
[b] Department of Materials Engineering, KU Leuven, B-3001 Heverlee, Belgium
[c] Department of Separation Science, LUT University, Mukkulankatu 19, 15210 Lahti, Finland
[d] Faculty of Medicine and Health Technology, Tampere University, Tampere, Finland

ARTICLE INFO

Keywords:
A. Natural fibres
B. Interface/interphase
B. Impact behaviour
E. Surface treatments

ABSTRACT

The application of natural flax fibre/epoxy composites is growing in the automotive sector due to their good stiffness and damping properties. However, the impact damage resistance of flax/epoxy composites is limited due to the brittle nature of both epoxy and flax fibres and strong fibre/matrix adhesion. Here, biobased thermoplastic cellulose acetate (CA) is deployed as a fibre treatment to alter the damage development of flax/epoxy composites subjected to low-velocity impact. The perforation threshold energy and the perforation energy of unmodified cross-ply composites increased respectively by 66% and 42% with CA-treated flax fibres. The CA-modification modestly decreased the transverse tensile strength and in-plane tensile shear strength of the composites. However, it altered the brittle nature of flax/epoxy laminates in quasi-static tests into ductile failure with clearly increased fibre–matrix debonding.

1. Introduction

Natural fibres, such as flax, are a class of green fibre reinforcements widely used in the semi-structural composite parts of the automotive and construction sectors [1–3]. Natural fibre composites offer low density as well as excellent damping properties and ecological merits [1,4]. Currently, flax is the only engineering plant fibre in Europe mass-produced in unidirectional and continuous fibre mats [1,5]. Epoxy resins are appealing for the industry based on their high mechanical properties and low viscosities, which are ideal for composites processing. Due to the reactive nature of epoxies, epoxy resins and natural fibres show good fibre/matrix adhesion with hydrogen and covalent bond formation [6]. The lower strength of natural fibres compared to synthetic fibres [7–9], combined with their relatively low strain to failure and the brittle nature of epoxy resins, limit the application of these flax biocomposites in environments where dynamic loads, such as impacts, are expected [10].

Low-velocity impacts (induced, for instance by collision, and dropped tools) can severely affect the further application, i.e. in terms of long term durability, of flax/epoxy composites by generating through-thickness damage in the form of matrix cracking, fibre failure and delamination [11,12]. For example, a 10 J low-velocity impact on flax/epoxy composite with $[0/90/+45/-45]_{2s}$ lay-up, a laminate thickness of 2.85 mm, and fibre volume fraction (V_f) of 44% can reduce its residual compressive strength by 30% [13]. Matrix toughness, stacking sequence, and flax fibres architecture are critical factors for proper impact damage tolerance of flax/epoxy composites [10,14]. Due to the relatively low strength of flax fibres and high interfacial shear strength of flax/epoxy [7], the impact damage pattern of flax/epoxy composites is usually dominated by fibre failure, shear-induced matrix cracks and limited delamination [12,13,15].

It is known that cross-ply composites based on UD plies absorb higher impact energies than ones based on woven plies due to the higher in-plane strength of cross-ply composites based on UD plies and because of much higher energy absorption due to delamination between the plies [16]. Nevertheless, cross-ply composites based on woven reinforcements exhibit limited damage compared to cross-ply laminates based on UD plies and thus tend to have better properties after impact (damage tolerance). This is due to the coarse fibre bundles within the woven fabrics that act as crack-stoppers and because of reduced delamination

* Corresponding author.
E-mail address: farzin.javanshour@tuni.fi (F. Javanshour).

https://doi.org/10.1016/j.compositesa.2021.106628
Received 13 April 2021; Received in revised form 31 May 2021; Accepted 22 August 2021
Available online 25 August 2021

due to nesting of the woven fabrics [16,17]. For dissimilar ply angles, specifically cross-ply configurations (with either UD or woven reinforcements), the composites' tendency to delaminate at the interface between non-aligned fibre plies can be affected by the mismatch of bending stiffness between adjacent plies [18].

By presuming that flax/epoxy composites can be designed so that the impact damage can be restrained, it might be possible to limit the loss in residual strength and finally replace the 'no damage growth' design by limited damage growth designs, which can save substantial amounts of material and energy. For this, the composites' interfacial toughness should be engineered to suppress damage growth, especially near the laminate mid-plane as the most critical failure location [19].

The literature on interfacial and interlaminar toughening of flax/epoxy composites focusing on impact resistance is minimal [20–22]. Ravandi et al. [23] reported a detrimental effect of stitching on interlaminar toughness and low-velocity impact resistance of flax/epoxy composites due to fibre distortion and resin-rich pockets. Prasad et al. [21] reported that the addition of TiO_2 to epoxy resin improves the mode I and mode II fracture toughness of flax/epoxy composites by 52% and 73%, respectively, due to crack deflection/blunting near fibre/matrix interfaces. However, they did not study the contribution of TiO_2 to the impact resistance of composites. Gassan et al. [22] and Koolen et al. [20] evaluated the effect of a silicone-rich interface on the properties of flax fibre composites. Gassan et al. [22] reported an increase of Charpy impact strength of composites by 100% with an expense of 50% reduction in the flexural modulus and strength of the composites. Koolen et al. [20] hypothesised that interfacial toughening by the insertion of a thin silicone elastomer might improve the resistance to hygroscopic ageing. However, the fibre coating did not have the desired effect since an accelerated reduction of the transverse strength of UD flax-epoxy composites and increased fibre–matrix debonding after ageing indicated a weaker interface. This observation was explained by premature adhesive or cohesive failure in the silicone interlayer, which stresses the importance of material selection. An alternative route to mitigate the low impact resistance of fibre reinforced epoxy composites is to coat a thin layer of tough thermoplastic into the fibre/matrix interface [24–29]. For instance, Lin et al. [24] showed that 1.39% fibre sizing content of thermoplastic polyurethane improved the apparent fibre/matrix interfacial shear strength of aramid/epoxy by 67.7% as the ductile interface had higher deformation and delayed the debonding by crack deflection. Narducci et al. [25] suppressed and controlled the delamination growth of carbon/epoxy composites by polylactic acid based surface modification of carbon fibres.

In this study, the flax fibre surface was modified with fully biobased cellulose acetate (CA) thermoplastic coating to enhance flax/epoxy composites' interfacial toughness. The aim was to limit fibre failure and suppress primary delamination during the low-velocity impact of flax/epoxy laminates while preserving optimised quasi-static performance. CA is selected based on its excellent compatibility with flax fibre and epoxy resin, being green and cost-effective, and having high ductility (failure strain 13.5 ± 3%) and good mechanical properties [30].

The surface chemistry and morphology of CA treated flax yarns were characterised with Fourier transform infrared spectroscopy (FTIR) and scanning electron microscopy (SEM). The mechanical properties (tensile and bending resistance) of flax yarns were compared with those of CA modified flax yarns. Composites' mechanical performance under various loading conditions was evaluated by applying quasi-static tensile testing, short beam bending tests, and drop-weight impact analysis.

2. Methodology

Bcomp (Fribourg, Switzerland) provided non-crimp flax yarn fabric of unidirectional (UD) type 5009 with an areal density of 300 g/m^2. Pure cellulose acetate (CA) powder (average MW 100,000) was supplied by Acros Organics (New Jersey, United States). The degree of substitution of CA was 1.3. Technical acetone by Kiilto Oy (Lempäälä, Finland) was used as a solvent for CA powder. Standard epoxy resin Epopox A28 by Amroy Europe Oy (Lahti, Finland) and a Jeffamine D-23 polyether diamine hardener by Huntsman (Texas, USA) with 35 wt% hardener to resin ratio were used as the matrix polymer system.

Flax fabrics were modified with CA by dip-coating into a CA-acetone solution of 5% CA concentration (5 g CA in 100 mL acetone) as described in Supplementary data (S.1.1). CA, based on its acetyl content and degree of substitution, can dissolve in various solvents such as acetone, chloroform, 2-methoxyethanol, and dichloromethane. In this study, acetone was selected as a solvent, based on an extensive review on the green solvent guides by Byrne et al. [31], which categorised solvents into six subgroups from green (e.g. ethanol, water), between green and problematic (e.g. acetone), problematic (e.g. DMSO), between problematic and hazardous (e.g. dichloromethane), hazardous (e.g., 2-methoxyethanol), and highly hazardous (e.g. chloroform). Compared to other CA-solvents, acetone has the best environmental, health, safety, and energy demand and can be sourced renewably [31]. Also, dip-coating of flax fabrics in acetone solution is an energy-efficient and cost-effective method as it does not require specialised devices and an oven to evaporate the solvent.

The untreated and CA-modified flax fabrics and pure CA film were analysed by Fourier transform infrared (FTIR) spectroscopy (Perkin-Elmer Spectrum One, Perkin-Elmer, Beaconsfield, UK). The morphology of the fabrics was examined with an ULTRAplus (Zeiss, Oberkochen, Germany) scanning electron microscope (SEM). A thin gold coating was used to ensure enough conductivity for the SEM samples. The bending resistance of untreated and modified (as a flax-CA 'preform fabric') strips of UD flax fabrics was studied with a L&WTM bending resistance tester (Lorentzen & Wettre, Sweden). The test was performed according to the SCAN-P 29:95 standard (samples were 38 mm in width and 70 mm in length). Further descriptions of the bending resistance test are described in Supplementary data (Fig. S1). Transverse strength of UD CA-flax fabrics ('preforms') was tested with a universal tester (Instron 5967, MA, USA) with 500 N load cell, gauge length of 50 mm and a crosshead speed of 1 mm/min. The samples were 15 mm in width and 150 mm in length. The thickness of the fabrics was determined by the average thickness at three points along the gauge length. Masking tape was used as tabs at the gripping area. The polyester weft threads of the fabrics were removed before testing. The average results of ten samples were reported for bending resistance and transverse fabric tests.

Composite panels of flax/epoxy and CA-flax/epoxy with a fibre volume fraction (V_f) of 40% were manufactured based on the manual lay-up method (Supplementary data, S.1.3). The bulk density of composites was measured based on the Archimedes principle [32] (as described in Supplementary data S.1.4). The V_f and composites' morphology were characterised by X-ray computed tomography (Phoenix Nanotom, General Electric, Germany) as described in Supplementary data (S.1.5). The quasi-static tensile performance of composites with $[0]_4$ and $[\pm45]_s$ lay-ups was studied according to ASTM D3039 and ASTM D3518 standards, respectively. The effect of CA surface modification on fibre/matrix adhesion was studied based on transverse tensile strength tests of $[90]_4$ composites (ASTM D3039 standard) and short-beam testing of $[0/90]_{3s}$ composites (ASTM D2344 standard). The testing specifications are reported in Supplementary data (Table S1). The impact strength of UD ($[0]_4$ lay-up) CA-flax/epoxy and flax/epoxy were comparatively studied by a Ceast Resil 5.5 Charpy impact tester (Ceast, Torino, Italy) according to EN ISO 179–1 standard. The impact performance of structural flax/epoxy and CA-flax/epoxy composites, with a $[0/90]_{3s}$ lay-up, was studied with a drop-weight test (per ASTM D7136 and ASTM D5628 standards), without rebound impacts. To present a range of damage (e.g. local ply splitting/delamination for low impact energies to complete perforation of the specimen at the upper bound energy), the drop height was adjusted to 0.11, 0.22, 0.32, 0.44, 0.55, 0.66, 0.77, 0.88, 0.99, and 1.11 m to target the kinetic energies of 3, 6, 9, 12, 15, 18, 21, 24, 27, and 30 J, respectively; the mass of the impactor was 2772 g. Further specifications of the impact testing and the

relevant terminology are presented in Supplementary data (S.1.6). The post-impact assessment of failure mechanisms in the impacted specimens was evaluated with a DM 2500 M (Leica, Wetzlar, Germany) optical microscope using a dark field mode. The samples were embedded in an epoxy resin before polishing. The surface deformations on the backface of composites (opposite to the impacted surface after the drop-weight test) were inspected with three-dimensional optical profilometry with an InfiniteFocus G5 (Alicona, Graz, Austria).

3. Results and discussions

3.1. Fibre surface characterisation

Fig. 1 shows the FTIR transmittance spectra of untreated flax and CA-modified flax fibres. The FTIR spectrum of the flax fibre shows the typical vibration bands of cellulose, hemicellulose, and lignin, as reported previously [33]. The–OH stretching vibration (mainly related to cellulose) band of hydroxyl groups [34] in CA, flax fibre and CA-flax fibre appeared as broadband with the highest intense band positions 3490 cm^{-1}, 3344 cm^{-1} and 3357 cm^{-1}, respectively. It is clear from the figure that the –OH stretching vibration band of CA-flax fibre is shifted to the higher wavenumber with respect to neat flax fibre. It indicates strong intermolecular hydrogen bonding between the hydroxyl group of flax fibre and CA. The pure CA spectrum reveals characteristic peaks at 1735 cm^{-1} and 1221 cm^{-1} related to the stretching vibration of the C═O bond of ester groups and C—O bond of the ether group, respectively [34]. These distinct CA (C═O and C—O) peaks are shifted to 1740 cm^{-1} and 1232 cm^{-1} in CA-modified flax fibres, indicating hydrogen bonding between the C═O and C—O groups of CA and the hydroxyl group of flax.

SEM images, in Fig. 2, compare the morphology of flax and CA-flax yarns. A distinctive coating is evident on the CA-modified flax yarns, which bonds flax fibres together into a kind of flax-CA preform. SEM images of modified flax yarns show the thickness of CA coating to be ≈3μm. In Supplementary data (Table S3), CA-flax preforms show significantly higher bending resistance (442 ± 22 mN) than unmodified flax preforms (4 ± 1 mN). The CA-flax preforms possessed a transverse tensile strength of 268 ± 24 kPa, whereas flax preforms had no measurable transverse tensile strength. The tensile rupture force was similar for flax and CA-flax yarns (Supplementary data, Table S3 and Fig. S2). These results show that flax fibres have good compatibility with CA, and a uniform CA film can be achieved by dip-coating flax fabrics in CA-acetone solution. Furthermore, the CA bonds the flax fibres/yarns together so that it has enough structural integrity to be regarded as a flax-CA preform fabric.

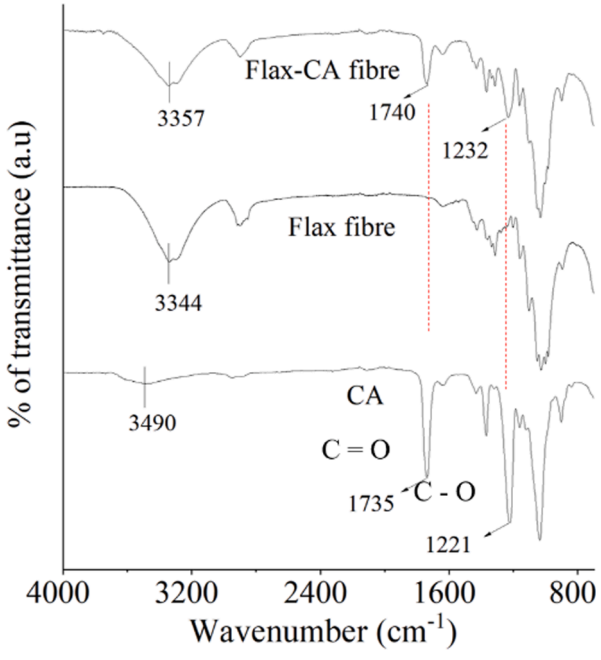

Fig. 1. FTIR transmittance spectra of untreated flax and CA-modified flax fibres. (For interpretation of the references to colour in this figure legend, the reader is referred to the web version of this article.)

3.2. Composites

3.2.1. Morphological properties

In Fig. 3, the morphology of UD flax/epoxy and CA-flax/epoxy composites is compared. The CA-flax/epoxy presents a well-organised ply architecture, and the spacing between yarns and plies is consistent. The distribution of flax yarns within flax/epoxy is relatively random, and resin-rich areas (without fibre) are more extensive than in CA-flax/epoxy. The more organised ply architecture of the modified composites can be due to the higher stiffness of the CA-flax fabrics than of the unmodified UD flax fabrics. Better flax fibre distribution within the CA-flax/epoxy composites with a lower amount of resin-rich areas can improve the ultimate behaviour of composites, such as fatigue and impact resistance where resin-rich areas can negatively affect the damage onset [23,35]. Both composites had a similar fibre volume fraction (40%) and densities (1.21 ± 0.30 g/cm^3).

3.2.2. Quasi-static tensile properties

Table 1 compares the quasi-static tensile performance of the prepared composites. The flax/epoxy and the CA-flax/epoxy composites with a $[0]_4$ lay-up have almost the same longitudinal chord modulus of elasticity (below 0.1% strain) in the range of 25 GPa and ultimate tensile strength in the range of 260 MPa, respectively. The ultimate tensile strain of the CA-modified laminates in the longitudinal and transverse directions to the fibre direction are respectively 13% and 39% higher than the corresponding values for the flax/epoxy; in the 45° orientation, the failure strain is even 52% higher.

Fig. 4 A, B show the longitudinal tensile stress–strain plots for flax/epoxy and CA-flax/epoxy laminates exhibiting very similar behaviour of the composites. As shown in Fig. 4 B, the brittle failure mode of UD flax/epoxy composites (transverse to fibre direction) changes into a more ductile shear-type of failure along the fibre direction in CA-modified composites, which is a favourable failure type in many structural applications. The failure along the fibre direction in longitudinal tensile tests shows better interfacial toughness [19].

Fig. 4 C shows the representative stress–strain behaviour of the composites under transverse ($[90]_4$ lay-up) loading condition. The CA-modified composite had ≈13% lower transverse tensile strength than the flax/epoxy version. The fibre/matrix adhesion between flax and epoxy is partly based on covalent/hydrogen bonding [33]. In CA-flax/epoxy, the adhesion is based on hydrogen bonding between flax and CA-coating and covalent/hydrogen bonding between CA-coating and epoxy resin, in addition to some microscale mechanical interlocking. The presence of only hydrogen bonding between CA-flax can be the reason for the lower transverse strength of CA-flax/epoxy. Similarly, Koolen et al. [20] assigned the reduction in transverse strength of UD flax composites having a silicone rich interface to the poor adhesion between the silicone coating and epoxy matrix, which relies solely on Van der Waals forces and few chemical bonds. The transverse tensile modulus for flax/epoxy and CA-flax/epoxy composites are similar in their value (a bit more than 4 GPa). However, CA-modified composites exhibit a 39% higher transverse failure strain (compared to unmodified flax/epoxy), which can increase the damage tolerance of composites [36]. The comparison between transverse tensile fracture surfaces of flax/epoxy (in Fig. 5) and CA-flax/epoxy (in Fig. 6) provides further insight. In Fig. 5, the fracture surface of unmodified flax/epoxy is matrix dominated (cohesive) without fibre failure as expected. The residual epoxy on flax yarns in Fig. 5 A shows good fibre/matrix adhesion. In

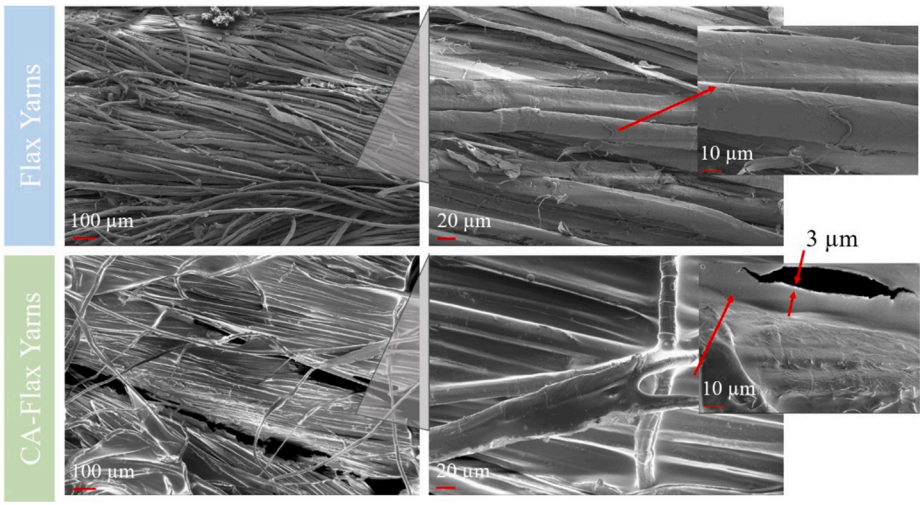

Fig. 2. SEM images of untreated and CA-treated flax yarns. (For interpretation of the references to colour in this figure legend, the reader is referred to the web version of this article.)

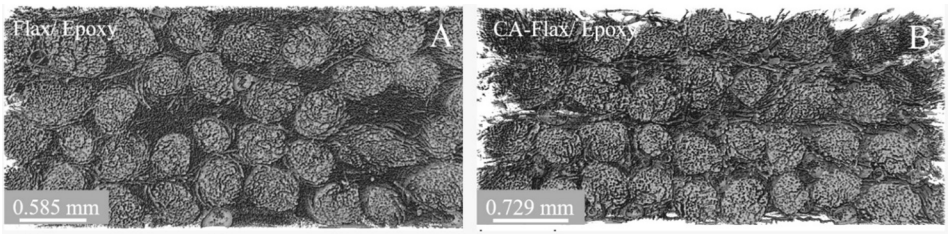

Fig. 3. Morphology of (A) UD flax/epoxy and (B) CA-flax/epoxy composites based on the µCT scans.

Table 1
Quasi-static tensile properties of the flax/epoxy and the CA-flax/epoxy composites.

Lay-up	Fibre	$E_{(0.1\%)}$ (GPa)	$\sigma_{Ultimate}$ (MPa)	$\varepsilon_{Ultimate}$ (%)	Tensile toughness (MJ/m^3)
$[0]_4$	Flax	24.98 ± 0.85	260 ± 7	1.66 ± 0.04	23.8 ± 1.1
	CA-Flax	24.55 ± 0.56	260 ± 11	1.88 ± 0.07	26.6 ± 1.6
$[90]_4$	Flax	4.51 ± 0.52	18.58 ± 1.54	0.49 ± 0.14	0.6 ± 0.1
	CA-Flax	4.22 ± 0.74	16.41 ± 1.31	0.68 ± 0.13	0.7 ± 0.1
$[\pm45]_s$	Flax	5.21 ± 0.25	67 ± 2	3.72 ± 0.49	19.2 ± 4.5
	CA-Flax	4.82 ± 0.43	52 ± 5	5.64 ± 0.37	23.6 ± 4.3

Fig. 5 B-D, the mirror-like (without texture) surface of epoxy in the interlayer regions shows the brittle nature of failure [19].

In Fig. 6 A, the transverse tensile fracture surface of CA-flax/epoxy demonstrates a preferential fracture at the fibre/matrix interface, unlike flax/epoxy. The presence of fibre imprints and flax yarns without bulk epoxy residuals indicates weaker fibre/matrix adhesion than for unmodified flax/epoxy. In Fig. 6 B-D, scarps (cleavage steps) are evident at the fracture surface of epoxy in the interlayer regions, which shows the progressive nature of failure contrary to unmodified flax/epoxy. The progression and coalescence of microcracks starting from the fibre debonding sites dissipates energy by creating new surfaces and delays the failure of composites [19] which explains higher elongation at failure and plasticity of CA-flax/epoxy compared to unmodified flax/epoxy. In Fig. 4 D, there is a comparison of the in-plane shear behaviour of unmodified and CA-modified flax/epoxy composites with a $[\pm45]_s$ lay-up. Both composites indicate similar initial stiffness of around 5 GPa. The ±45° tensile strength of CA-flax/epoxy (52 ± 5 MPa) is manifested by extensive interlaminar and intra-ply shear failure. For flax/epoxy (indicated ±45° tensile strength 67 ± 2 MPa), the failure mode is not dominated by shear modes but by brittle fibre failure (as visible in the micrographs of Fig. 4 D). The achieved increase in the overall shear toughness is evident from the dissipated fracture energy (comparison from integrated areas under stress–strain curves) that is 23.9 ± 6.8% higher compared to the non-modified composite. The ultimate failure strain is 52% higher for CA-flax/epoxy (5.64 ± 0.37%) compared to flax/epoxy (3.72 ± 0.49%).

Fig. 7 A, B show the brittle failure mode of flax/epoxy composites dominated by fibre failures with minor shear deformation and the mirror-like surface of epoxy within the interlayer regions. Fig. 7 C, D show the fracture surfaces of CA-flax/epoxy after $[\pm45]_s$ tensile test. In Fig. 7 C, the characteristic shear induced deformation of epoxy along the fibre direction (known as cusp features) and fibre imprints are evident, which indicate failure mainly based on shear loading [19]. Contrary to the mirror-like texture of epoxy in flax/epoxy, the cleavage marks of epoxy (known as scarps) are visible in Fig. 7 D, indicating the progressive failure of CA-flax/epoxy and further dissipation of energy. So, the CA modification allows extensive plastic deformation in shear for both interlaminar and intra-ply modes. In summary, tensile toughness (area under stress–strain curve) of CA-flax/epoxy composites with longitudinal ($[0]_4$) configuration is 11.6 ± 1.4 % higher than for unmodified flax/epoxy composites while both composites show similar transverse tensile ($[90]_4$) toughness (Table 1). Specifically, CA-surface modification significantly improves the tensile toughness of composite laminates subjected to in-plane shear loading. These improvements are further anticipated to lead to better impact damage resistance.

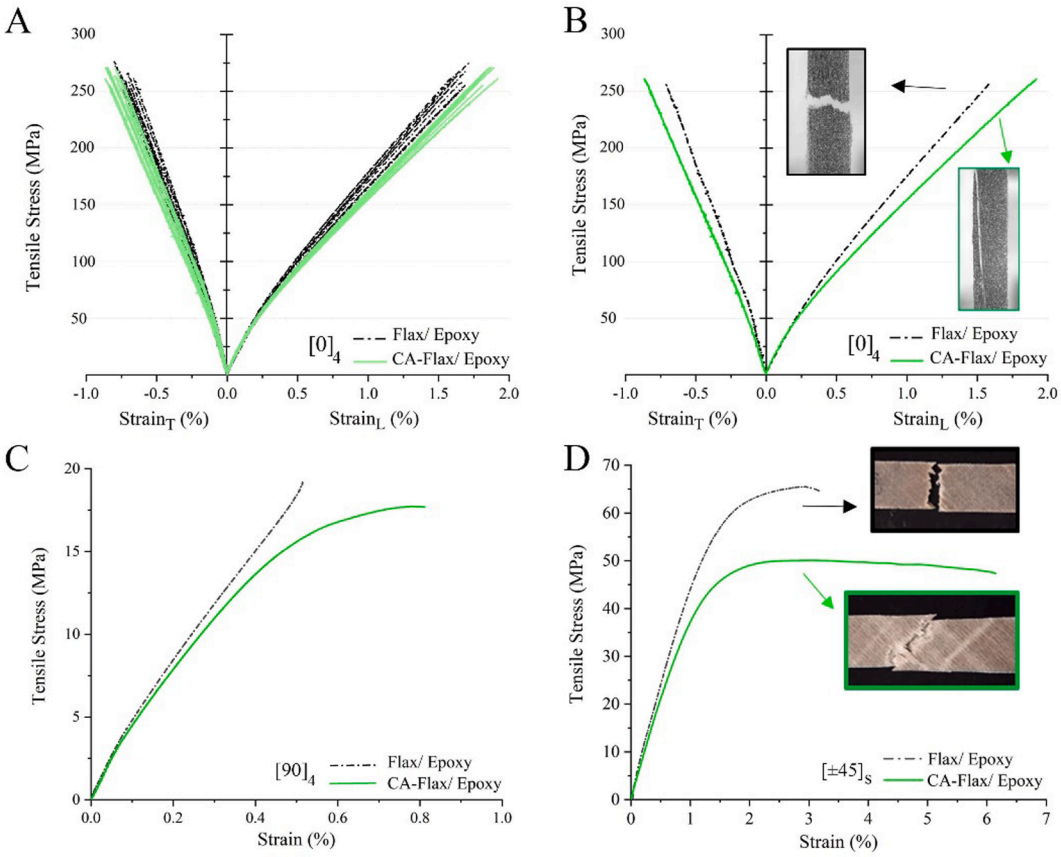

Fig. 4. Quasi-static stress–strain results. Plot A shows all longitudinal test results, and plots B, C, D are examples of the typical, representative curves for longitudinal, transverse and ±45° tensile tests. (For interpretation of the references to colour in this figure legend, the reader is referred to the web version of this article.)

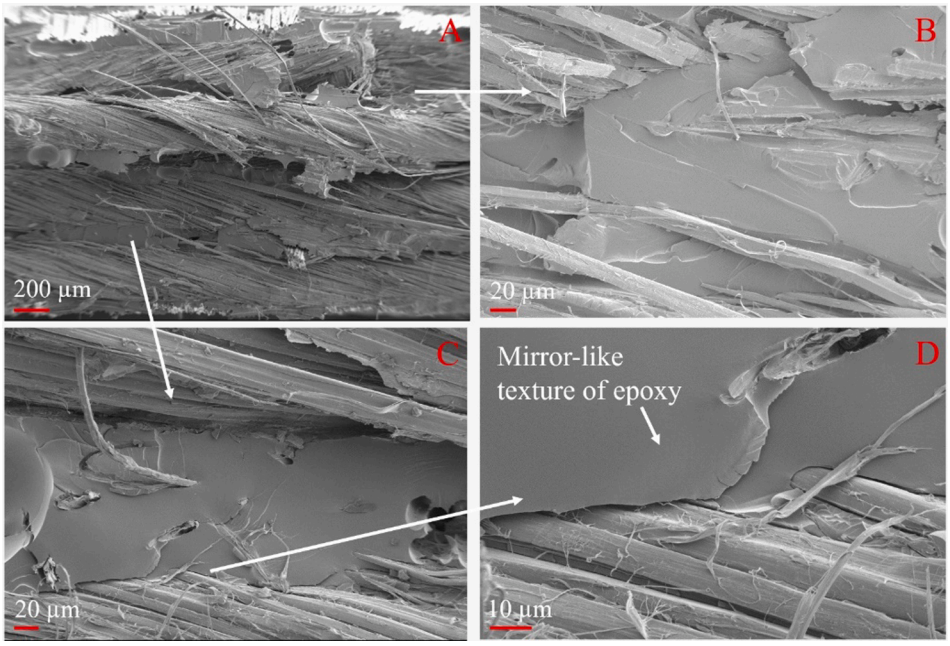

Fig. 5. The transverse tensile fracture surface of flax/epoxy (A, B, C, D). (For interpretation of the references to colour in this figure legend, the reader is referred to the web version of this article.)

3.2.3. *Flexural performance*

Fig. 8 presents short-beam shear stress-displacement curves for flax-epoxy and CA-flax/epoxy composites with a $[0/90]_{3s}$ lay-up. The apparent interlaminar shear strength (ILSS) of flax/epoxy (27.41 ± 0.44 MPa) was 17% higher than for CA-flax/epoxy (23.27 ± 0.53 MPa). Thermoplastic surface modification of flax fibres with CA changed the

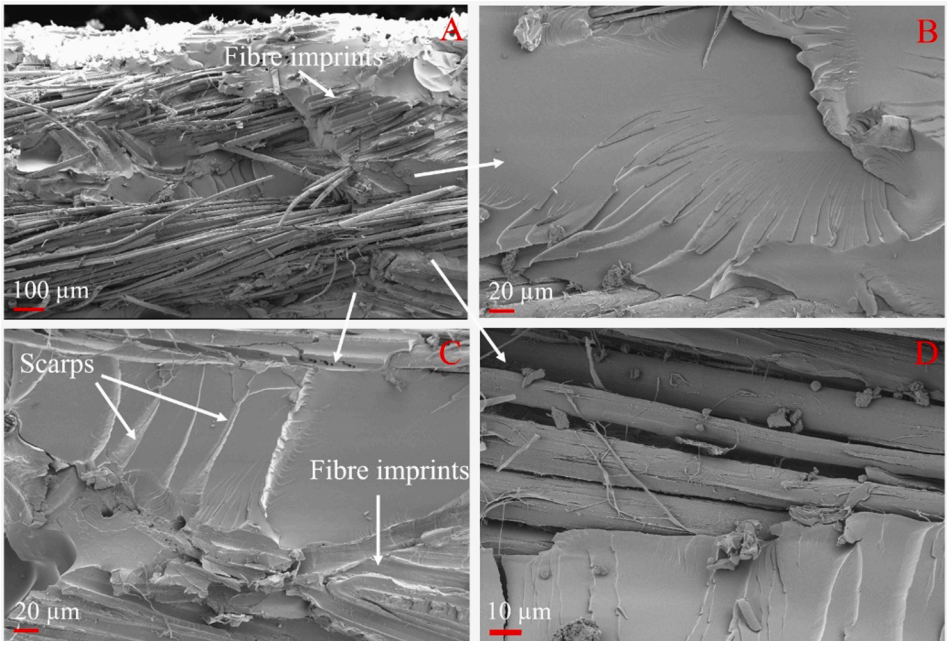

Fig. 6. The transverse tensile fracture surface of CA-flax/epoxy (A, B, C, D). (For interpretation of the references to colour in this figure legend, the reader is referred to the web version of this article.)

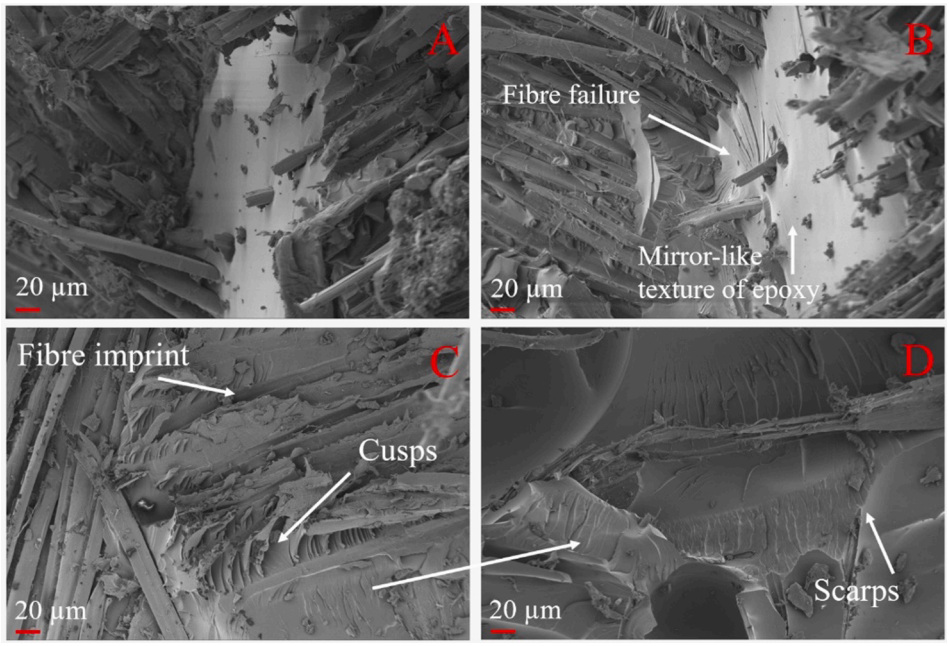

Fig. 7. The $[\pm 45]_s$ tensile fracture surface of flax/epoxy (A, B) and CA-flax/epoxy (C, D). (For interpretation of the references to colour in this figure legend, the reader is referred to the web version of this article.)

failure mode from fibre failure (at the tension/bottom side of the sample, as shown in Fig. 8 I) into fibre/matrix debonding and delamination (Fig. 8 II). CA-flax/epoxy follows a moderately progressive failure after reaching the ultimate load peak – resembled by a significant increase in ductility compared to the performance of flax/epoxy with a brittle failure mode. The step-like force (stress) drops in Fig. 8 are believed to occur due to local fibre–matrix debonding and delamination and local fibre failure. The dissipated energy upon short-beam flexure of CA-flax/epoxy (defined as the area under the short-beam force–displacement curve) was equal to 2.77 ± 0.29 J which was 95% higher than for flax/epoxy (1.42 ± 0.17 J). The improvement in the short-beam test energy dissipation of flax/epoxy composites with CA-coating can be beneficial for the damage tolerance of thin composite laminates subjected to local impact incidents. These results indicate that the CA-surface modification can impart a better toughness based on crack deflection due to increased debonding and spread of damage compared to flax/epoxy composites under flexural load.

3.2.4. *Impact performance*

Fig. 9 illustrates examples of the typical contact force-central displacement traces of the drop-weight impacted specimens (3 J, 18 J and 21 J energies) for the $[0/90]_{3s}$ lay-ups. In the initial loading phase,

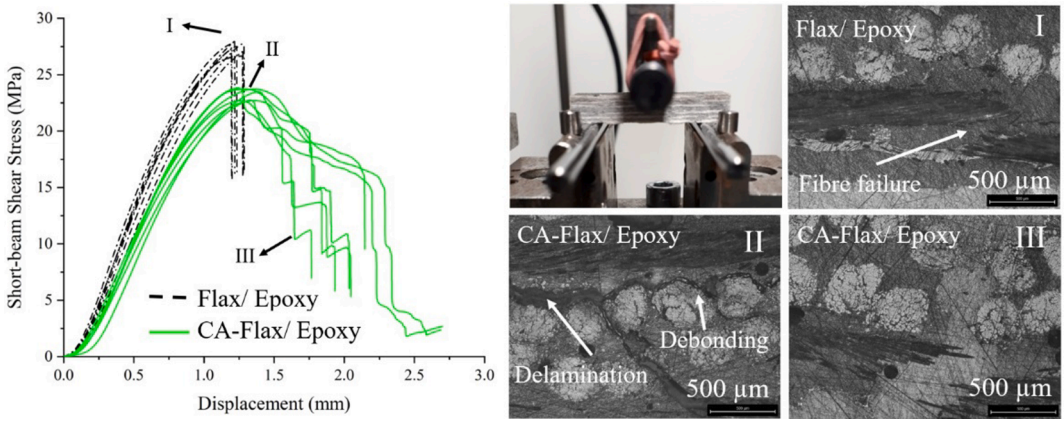

Fig. 8. Short-beam shear stress-displacement curves and failure mode analysis together with cross-sectional micrographs. (For interpretation of the references to colour in this figure legend, the reader is referred to the web version of this article.)

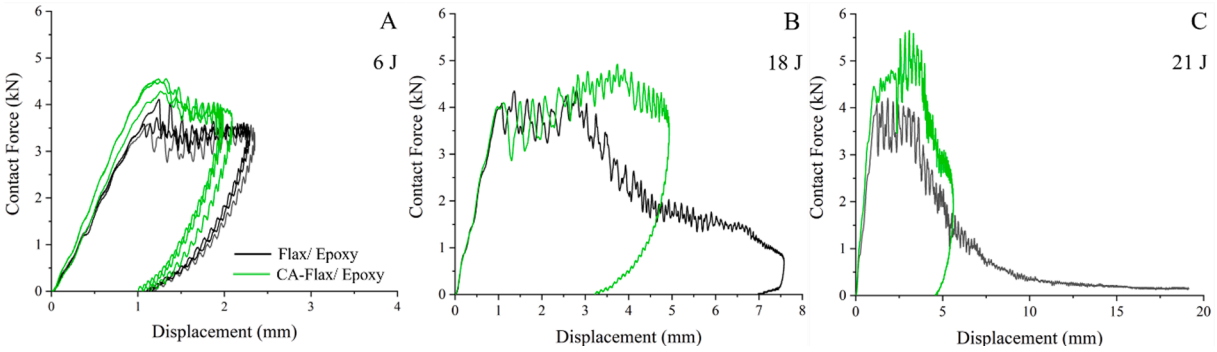

Fig. 9. Typical contact force-central displacement traces of the flax/epoxy and the CA-flax/epoxy composites at 6 J (A), 18 J (B), and 21 J (C) drop-weight impact energies. (For interpretation of the references to colour in this figure legend, the reader is referred to the web version of this article.)

contact force–displacement curves extend linearly from the origin towards the maximum force. The maximum contact force in drop-weight impact incident of composites indicates the resistance of specimens against impact event and mainly depends on fibre strength [8,10,16] and fibre dominated ultimate fractures [16]. Right after reaching the maximum force, shown in Fig. 9, the damages develop and propagate within the composite while the impactor still moves against the specimen until the movement stops at the turning/rebound point. The extension of the force fluctuations in the zone (between loading and rebound phases) is typically associated with various damages (e.g., delamination, shear-induced and bending induced matrix cracks, and fibre failure) [8,37]. The energy absorbed during the impact incident is equal to the enclosed area under the force–displacement curve (hysteresis loop), and the recovered (elastic) impact energy is equal to the difference between total impact energy (area before a rebound) and absorbed energy [38]. In the perforation impact incident, the specimen absorbs all the impact energy, and there is no recovered elastic impact energy like the contact force–displacement curve of unmodified flax/epoxy in Fig. 9 C.

In Fig. 9, the extent of damage (displacement within the fluctuation

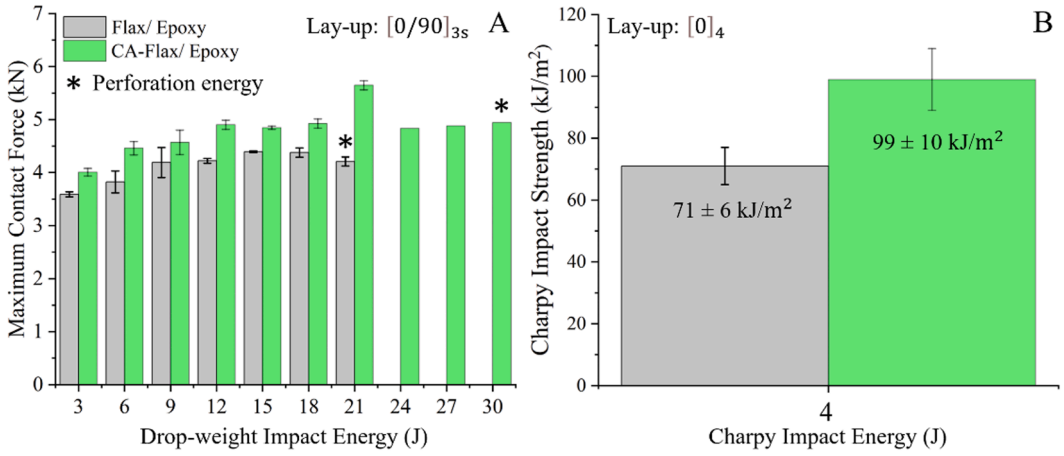

Fig. 10. Maximum drop-weight impact force (A) and Charpy impact strength (B) of composites. (For interpretation of the references to colour in this figure legend, the reader is referred to the web version of this article.)

phase) increases for tests with impact energies from 6 J to 21 J. The extent of damage progression within CA-flax/epoxy is lower than in the case of flax/epoxy. The lower damage progression indicates that the impactor encounters continuous, ductile resistance when penetrating the composite system due to the CA-flax/epoxy's higher toughness. Naturally, the suppressed impact damage of flax/epoxy with CA-surface modification is anticipated to enhance the post-impact-tested residual flexural/compression strength [10,13].

Fig. 10 A shows the maximum drop-weight contact force of composites subjected to impact energies from 3 J to perforation energy which is 21 J for unmodified flax/epoxy and 30 J for CA-flax/epoxy. The contact force of flax/epoxy got enhanced by 12% for all impact energy levels with CA-modification, which was expected according to the higher toughness of the CA-flax/epoxy composite (see Table 1). Likewise, in Fig. 10 B the Charpy impact strength of UD flax/epoxy composites with a $[0]_4$ lay-up was 71 ± 6 kJ/m^2, which got improved by 38% (to 99 ± 10 kJ/m^2) due to the CA-surface modification The brittle fracture mode of UD flax/epoxy composites related to the Charpy impact tests transformed into a combination of fibre debonding and delamination with the CA surface modification (as reported in Supplementary data, Fig. S4).

Fig. 11 A, B clearly show the contribution of CA-surface modification to the perforation resistance of flax/epoxy composites. The impactor's overall contact time with CA-flax/epoxy specimens is lower than for flax/epoxy specimens, which indicates that CA-modified composites have a better resistance against impacts – better overall elasticity under impact loading. After 15 J, flax/epoxy composite absorbed almost all the (initial) impact energy and transferred it into ply failure and, finally, complete perforation and almost no recovered elastic energy occurred at 21 J. Fig. 11 B shows that the CA-surface modification enhances the perforation energy of flax/epoxy by 42% to 30 J which is a significant contribution to the impact resistance and safety of flax/epoxy composites. Based on the results from tensile tests, tensile shear tests, and short beam flexural tests, the higher perforation energy of CA-flax/epoxy is due to the higher interfacial toughness and ductility of the CA-modified composite laminates.

Fig. 11 C, D compare the absorbed and recovered (elastic) impact energies, respectively. The absorbed energies of flax/epoxy and CA-flax/epoxy increase linearly with impact energies. Both composites have very similar absorption capability for energies of 3 J and 6 J. At 9, 12, 15, 18 and 21 J impact energies, the flax/epoxy, respectively, absorbed 1.7%, 4.6%, 7.7%, 8.5%, and 5% more impact energy than the CA-modified composite. The reason for the higher energy absorption of unmodified flax/epoxy is the greater extent of damage compared to CA-flax/epoxy [10,16]. The recovered (elastic) energy, shown in Fig. 11 D, increases linearly from 3 J to 9 J for modified and unmodified composite specimens. The recovered energy of flax/epoxy starts to decrease after the 9 J energy level to zero at 21 J, indicated by the final perforation of these reference composites. Based on Fig. 11 D, the perforation threshold energy (defined here as the point where recovered energy starts to degrade) shifts from 9 J (for flax/epoxy) to 15 J (66% improvement) with the CA thermoplastic fibre surface modification.

Fig. 12 presents typical damage patterns of flax/epoxy composites subjected to low-velocity impact. The majority of matrix cracks and local fibre failures are towards the rear-face, and shear induced matrix cracks are seen near the mid-plane of composites [10,37], similar to Fig. S7 and Fig. S8 micrographs in the supplementary data.

Fig. 13 A compares the damage in flax/epoxy and CA-flax/epoxy specimens subjected to drop-weight impact incidents. Both flax/epoxy and CA-flax/epoxy specimens do not significantly damage after a 3 J

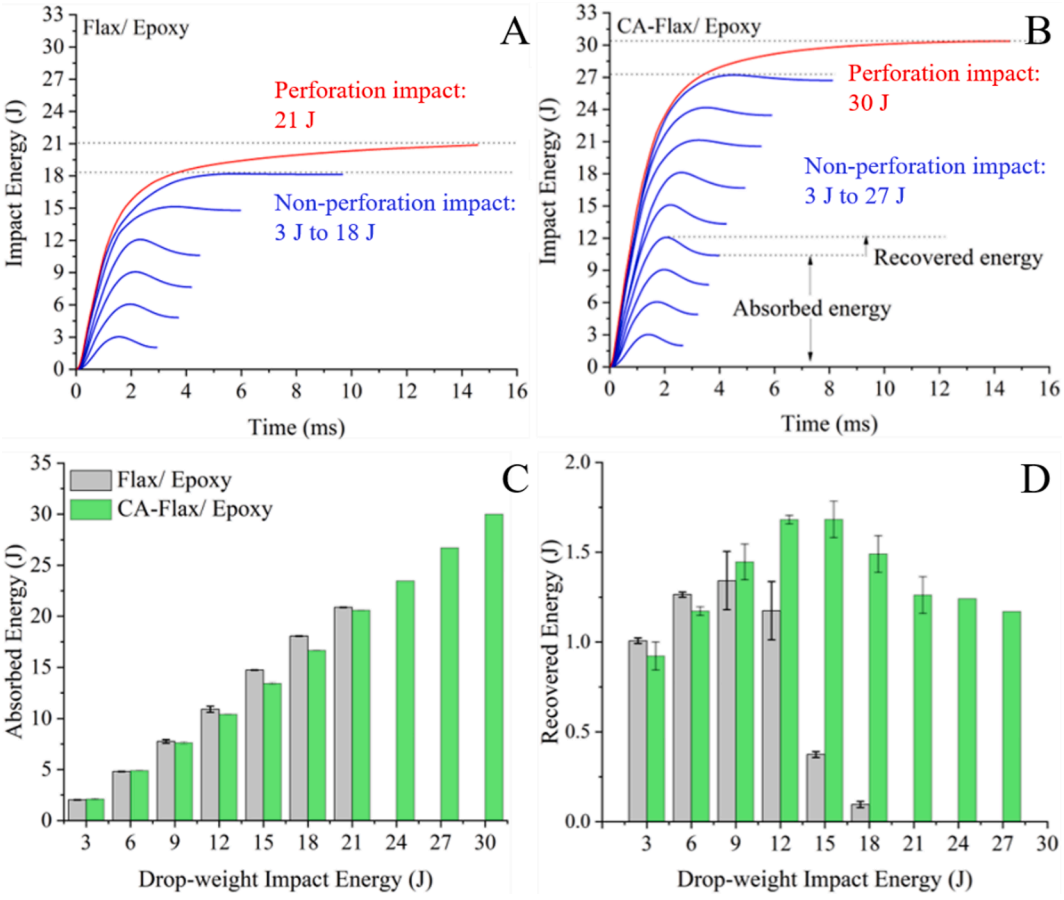

Fig. 11. Energy-time history of 3 J to complete perforation impact energies for flax/epoxy (A) and CA-flax/epoxy (B) composites and their corresponding absorbed energy (C) and recovered energy (D). (For interpretation of the references to colour in this figure legend, the reader is referred to the web version of this article.)

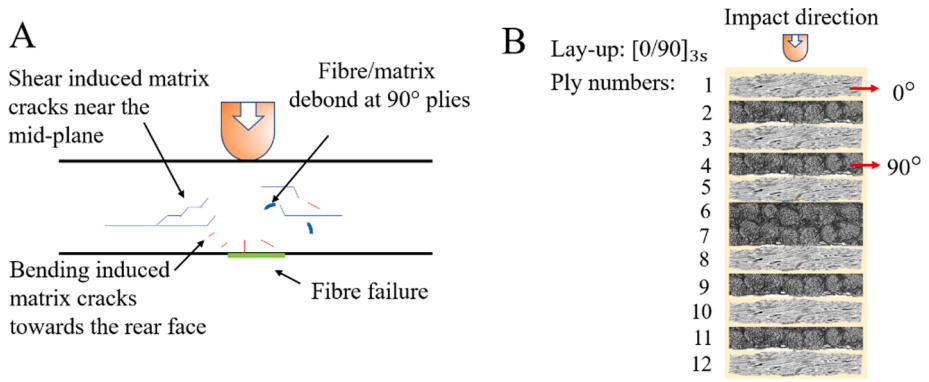

Fig. 12. Illustration of typical damage patterns of the flax/epoxy composites subjected to low-velocity drop-weight impact (A), and the composite cross-section before an impact test (B). (For interpretation of the references to colour in this figure legend, the reader is referred to the web version of this article.)

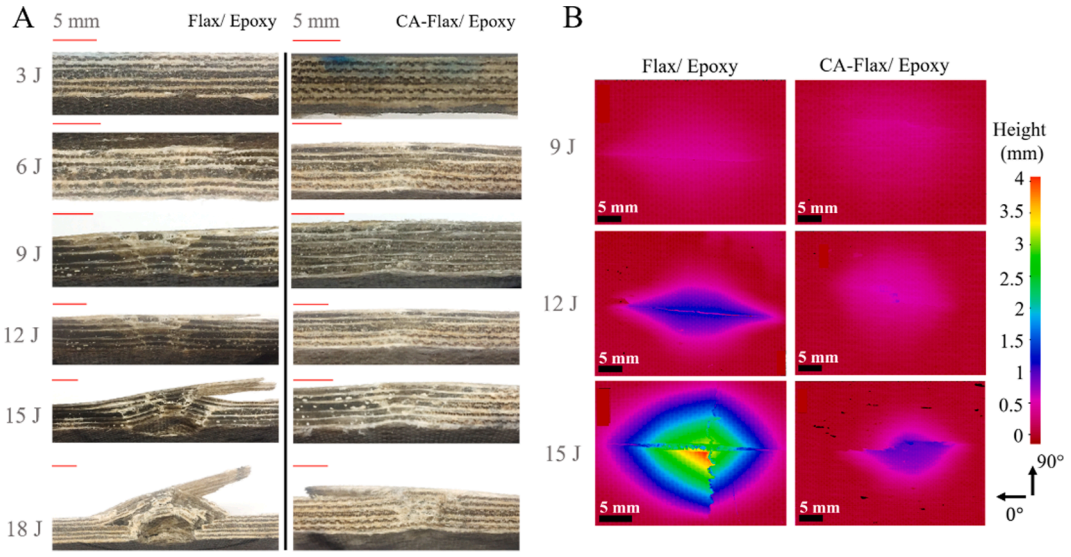

Fig. 13. A: Through thickness inspection of the flax/epoxy and CA-flax/epoxy specimens after 3 J to 18 J impact events. B: Profilometer images from rear-face surface permanent deformation after 9 J, 12 J, and 15 J impact events. The 3 J and 6 J impacts did not cause any deformation at the rear-face. (For interpretation of the references to colour in this figure legend, the reader is referred to the web version of this article.)

impact except for minor matrix cracks on the composites' rear-face (12th ply defined in Fig. 12 B). After the 6 J impact, a fibre failure is evident at the rear-face of the flax/epoxy specimen, but no damage is visible for CA-flax/epoxy (detailed microscopy images are available in the Supplementary data, Fig. S7). After 9 J and 12 J impacts, shear-induced matrix cracks near mid-plane were noted for flax/epoxy (being more severe for higher energy impact), but only local fibre/matrix debonds at 6th and 7th plies were visible for CA-flax/epoxy. These

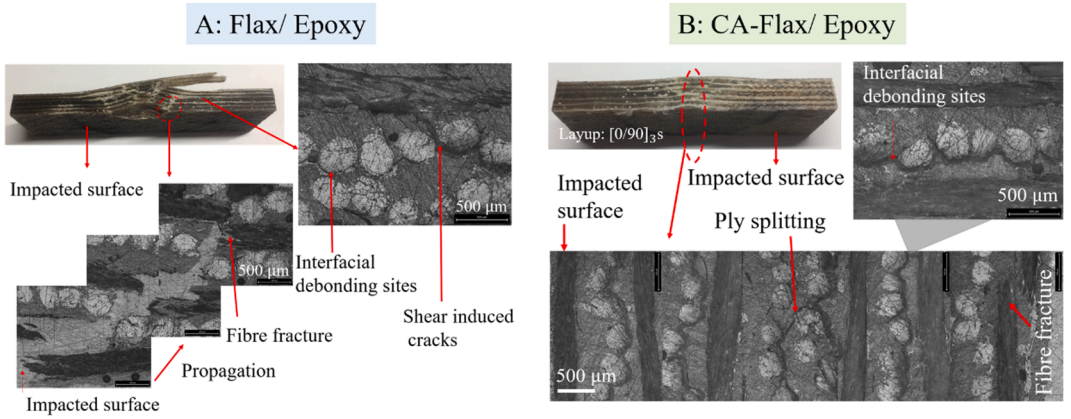

Fig. 14. Through thickness damage patterns of flax/epoxy (A) and CA-flax/epoxy (B) specimens after 15 J drop-weight impact incident. (For interpretation of the references to colour in this figure legend, the reader is referred to the web version of this article.)

damages are visible in microscopy images in Supplementary data (Fig. S8). In Fig. 13 B, the permanent surface deformation at the rear-face of flax/epoxy (based on the profilometer surface measurement on 12th ply) is increased from 0.5 mm after the 9 J impact incident to 2 mm after the 12 J impact, which is considerably higher than for CA-flax/epoxy specimens.

Fig. 14 compares in more detail the damage of flax/epoxy and CA-flax/epoxy specimens after 15 J impacts. Flax/ epoxy specimen experiences a six ply breakage, interfacial debonding, and ply splitting. However, CA-flax/epoxy specimens exhibited only fibre failure at the rear-face and fibre/matrix debonding at 90° plies (namely 2nd, 4th, 6th, 7th, 9th, and 11th plies). The limited fibre breakage in CA-modified composites compared to unmodified ones corroborates with the higher recovered elastic energy of CA-flax/epoxy compared to flax/epoxy, especially at 12 J (by +43%), 15 (by +354%), and 18 J (by +1452%) impact energies in Fig. 11 D. The profilometer-measured rear-face surface deformations of unmodified and CA-modified flax/epoxy specimens after the 15 J impact test (in Fig. 13 B) correlate with the cross-sectional optical microscope images. Similar improvement with the CA surface modification was evident after the 18 J impact energy test. In toughened multi-axial cross-ply composites (with thermosetting resin), fibre splitting only appears within the outer ply (rear-surface) without extensive delamination and splitting on internal plies [16] as in the case of CA-flax/epoxy.

Our results showed that it is possible to control how the impact damage manifests itself in flax/epoxy composites from ply splitting and extensive fibre failure to fibre/matrix debonding (at 90° plies) and fibre failure at rear-face ply (Fig. 14). The findings showed that interfacial and interlaminar toughness plays a critical role in the damage resistance of flax/epoxy composites and agrees with previous reports for different composites [10]. This investigation revealed a potential to control natural fibre composites' impact damage progression with cellulose-based thermoplastic surface modification. Especially the 42% improvement in the perforation energy of cross-ply flax/epoxy composites with CA-surface modification can promote the further application of natural fibre composites in structural applications such as automotive, where impact resistance is critical. In future work, the fatigue performance of flax/epoxy composites will have to be analysed to understand further the quantitative toughening effects on dynamic load range and practical load spectra.

4. Conclusions

This paper presents a novel surface modification method to improve the interfacial toughness and low-velocity impact resistance of flax/epoxy composites by deploying thin (≈3 μm) and distinct biobased cellulose-acetate (CA) thermoplastic coating at the fibre surface. The CA-modification allowed extensive plastic deformation in shear for all quasi-static loading modes. Short-beam flexural testing showed a 17% decrease in apparent interlaminar shear strength of flax/epoxy composites with CA-modification. However, the CA-surface modification altered the brittle catastrophic failure of flax/epoxy composites into progressive failure with considerably larger energy dissipation based on crack deflection due to increased debonding and spread of damage. The maximum drop-weight impact contact forces of cross-ply CA-flax/epoxy laminates were 12% higher than for flax/epoxy for all the tested impact energies. Similarly, the Charpy impact strength of UD CA-flax/epoxy was 38% higher than for flax/epoxy. The CA-treatment enhanced perforation threshold energy and perforation energy of flax/epoxy by 66% and 42%, respectively. The CA-surface modification significantly improved the recovered (elastic) energy of flax/epoxy composites. The improvement in the recovered energy manifested itself with a lower extent of fibre failure. The surface modification presented in this investigation provides the potential to manipulate the damage progression due to dynamic loads, such as impact.

CRediT authorship contribution statement

F. Javanshour: Conceptualization, Methodology, Formal analysis, Investigation, Writing – original draft, Visualization. **A. Prapavesis:** Investigation, Formal analysis. **T. Pärnänen:** Investigation, Formal analysis. **O. Orell:** Investigation. **M.C. Lessa Belone:** Investigation. **R.K. Layek:** Writing – review & editing. **M. Kanerva:** Supervision, Methodology. **P. Kallio:** Funding acquisition. **A.W. Van Vuure:** Supervision, Funding acquisition. **E. Sarlin:** Investigation, Supervision, Funding acquisition.

Declaration of Competing Interest

The authors declare that they have no known competing financial interests or personal relationships that could have appeared to influence the work reported in this paper.

Acknowledgements

This project is funded by the European Union's Horizon 2020 research and innovation programme under the Marie Skłodowska-Curie grant agreement No 764713-FibreNet. This work made use of Tampere Microscopy Center facilities at Tampere University. The authors are grateful to Bcomp (Fribourg, Switzerland) for supplying the flax fabrics and providing valuable insights.

Appendix A. Supplementary material

Supplementary data to this article can be found online at https://doi.org/10.1016/j.compositesa.2021.106628.

References

[1] Bourmaud A, Beaugrand J, Shah DU, Placet V, Baley C. Towards the design of high-performance plant fibre composites. Prog Mater Sci 2018;97:347–408. https://doi.org/10.1016/j.pmatsci.2018.05.005.

[2] Zhang Z, Cai S, Li Y, Wang Z, Long Yu, Yu T, et al. High performances of plant fiber reinforced composites—A new insight from hierarchical microstructures. Compos Sci Technol 2020;194:108151. https://doi.org/10.1016/j.compscitech.2020.108151.

[3] Li Mi, Pu Y, Thomas VM, Yoo CG, Ozcan S, Deng Y, et al. Recent advancements of plant-based natural fiber–reinforced composites and their applications. Compos Part B Eng 2020;200:108254. https://doi.org/10.1016/j.compositesb:2020.108254.

[4] Duc F, Bourban PE, Plummer CJG, Månson J-A-E. Damping of thermoset and thermoplastic flax fibre composites. Compos Part A Appl Sci Manuf 2014;64:115–23. https://doi.org/10.1016/j.compositesa.2014.04.016.

[5] Corbin A-C, Sala B, Soulat D, Ferreira M, Labanieh A-R, Placet V. Development of quasi-unidirectional fabrics with hemp fiber: a competitive reinforcement for composite materials. J Compos Mater 2021;55(4):551–64. https://doi.org/10.1177/0021998320954230.

[6] Islam MS, Pickering KL, Foreman NJ. Influence of alkali fiber treatment and fiber processing on the mechanical properties of hemp/epoxy composites. J Appl Polym Sci 2011;119(6):3696–707. https://doi.org/10.1002/app.v119.610.1002/app.31335.

[7] Haggui M, El Mahi A, Jendli Z, Akrout A, Haddar M. Static and fatigue characterization of flax fiber reinforced thermoplastic composites by acoustic emission. Appl Acoust 2019;147:100–10. https://doi.org/10.1016/j.apacoust.2018.03.011.

[8] Barouni AK, Dhakal HN. Damage investigation and assessment due to low-velocity impact on flax/glass hybrid composite plates. Compos Struct 2019;226:111224. https://doi.org/10.1016/j.compstruct.2019.111224.

[9] Dhakal HN, Sarasini F, Santulli C, Tirillò J, Zhang Z, Arumugam V. Effect of basalt fibre hybridisation on post-impact mechanical behaviour of hemp fibre reinforced composites. Compos Part A Appl Sci Manuf 2015;75:54–67. https://doi.org/10.1016/j.compositesa.2015.04.020.

[10] Bensadoun F, Depuydt D, Baets J, Verpoest I, van Vuure AW. Low velocity impact properties of flax composites. Compos Struct 2017;176:933–44. https://doi.org/10.1016/j.compstruct.2017.05.005.

[11] Hull D, Yi BS. Damage mechanism characterisation in composite damage tolerance investigations. Compos Struct 1993;23(2):99–120.

[12] Ramakrishnan KR, Corn S, Le Moigne N, Ienny P, Slangen P. Experimental assessment of low velocity impact damage in flax fabrics reinforced biocomposites by coupled high-speed imaging and DIC analysis. Compos Part A Appl Sci Manuf 2021;140:106137. https://doi.org/10.1016/j.compositesa:2020.106137.

[13] Liang S, Guillaumat L, Gning PB. Impact behaviour of flax/epoxy composite plates. Int J Impact Eng 2015;80:56–64. https://doi.org/10.1016/j.ijimpeng.2015.01.006.
[14] Chew E, Liu JL, Tay TE, Tran LQN, Tan VBC. Improving the mechanical properties of natural fibre reinforced laminates composites through Biomimicry. Compos Struct 2021;258:113208. https://doi.org/10.1016/j.compstruct.2020.113208.
[15] Bensadoun F, Vanderfeesten B, Verpoest I, Van Vuure AW, Van Acker K. Environmental impact assessment of end of life options for flax-MAPP composites. Ind Crops Prod 2016;94:327–41. https://doi.org/10.1016/j.indcrop.2016.09.006.
[16] Schrauwen B, Peijs T. Influence of matrix ductility and fibre architecture on the repeated impact response of glass-fibre-reinforced laminated composites. Appl Compos Mater 2002;9:331–52. https://doi.org/10.1023/A:1020267013414.
[17] Awais H, Nawab Y, Anjang A, Md Akil H, Zainol Abidin MS. Effect of fabric architecture on the shear and impact properties of natural fibre reinforced composites. Compos Part B Eng 2020;195:108069. https://doi.org/10.1016/j.compositesb:2020.108069.
[18] Cantwell W. Geometrical effects in the low velocity impact response of GFRP. Compos Sci Technol 2007;67(9):1900–8. https://doi.org/10.1016/j.compscitech.2006.10.015.
[19] Greenhalgh ES. Failure analysis and fractography of polymer composites. Cambridge, UK: Woodhead Publishing Ltd.; 2009.
[20] Koolen G, Soete J, van Vuure AW. Interface modification and the influence on damage development of flax fibre - Epoxy composites when subjected to hygroscopic cycling. Mater. Today Proc., vol. 31, Elsevier Ltd; 2019, p. S273–9. https://doi.org/10.1016/j.matpr.2020.01.183.
[21] Prasad V, Sekar K, Varghese S, Joseph MA. Enhancing Mode I and Mode II interlaminar fracture toughness of flax fibre reinforced epoxy composites with nano TiO2. Compos Part A Appl Sci Manuf 2019;124:105505. https://doi.org/10.1016/j.compositesa.2019.105505.
[22] Gassan J, Dietz T, Bledzki AK. Effect of silicone interphase on the mechanical properties of flax-polyurethane composites. Compos Interfaces 2000;7(2):103–15. https://doi.org/10.1163/156855400300184262.
[23] Ravandi M, Teo WS, Tran LQN, Yong MS, Tay TE. Low velocity impact performance of stitched flax/epoxy composite laminates. Compos Part B Eng 2017;117:89–100. https://doi.org/10.1016/j.compositesb.2017.02.003.
[24] Lin J, Wang L, Liu L, Lu K, Li G, Yang X. Two-stage interface enhancement of aramid fiber composites: establishment of hierarchical interphase with waterborne polyurethane sizing and oxazolidone-containing epoxy matrix. Compos Sci Technol 2020;193:108114. https://doi.org/10.1016/j.compscitech.2020.108114.
[25] Narducci F, Lee KY, Pinho ST. Interface micro-texturing for interlaminar toughness tailoring: a film-casting technique. Compos Sci Technol 2018;156:203–14. https://doi.org/10.1016/j.compscitech.2017.10.016.
[26] Wu Z, Yi XS, Wilkinson A. Interlaminar fracture toughness of carbon fibre/RTM6-2 composites toughened with thermoplastic-coated fabric reinforcement. Compos Part B Eng 2017;130:192–9. https://doi.org/10.1016/j.compositesb.2017.08.003.
[27] Liu WenBo, Zhang S, Li B, Yang F, Jiao WeiCheng, Hao LiFeng, et al. Improvement in interfacial shear strength and fracture toughness for carbon fiber reinforced epoxy composite by fiber sizing. Polym Compos 2014;35(3):482–8. https://doi.org/10.1002/pc.v35.310.1002/pc.22685.
[28] Eyckens DJ, Randall JD, Stojcevski F, Sarlin E, Palola S, Kakkonen M, et al. Examining interfacial interactions in a range of polymers using poly(ethylene oxide) functionalized carbon fibers. Compos Part A Appl Sci Manuf 2020;138:106053. https://doi.org/10.1016/j.compositesa:2020.106053.
[29] Zhang Bo, Jia L, Tian M, Ning N, Zhang L, Wang W. Surface and interface modification of aramid fiber and its reinforcement for polymer composites: a review. Eur Polym J 2021;147:110352. https://doi.org/10.1016/j.eurpolymj.2021.110352.
[30] Uddin ME, Layek RK, Kim HY, Kim NH, Hui D, Lee JH. Preparation and enhanced mechanical properties of non-covalently-functionalized graphene oxide/cellulose acetate nanocomposites. Compos Part B Eng 2016;90:223–31. https://doi.org/10.1016/j.compositesb.2015.12.008.
[31] Byrne FP, Jin S, Paggiola G, Petchey THM, Clark JH, Farmer TJ, et al. Tools and techniques for solvent selection: green solvent selection guides. Sustain. Chem Process 2016;4(1). https://doi.org/10.1186/s40508-016-0051-z.
[32] Hallak Panzera T, Jeannin T, Gabrion X, Placet V, Remillat C, Farrow I, et al. Static, fatigue and impact behaviour of an autoclaved flax fibre reinforced composite for aerospace engineering. Compos Part B Eng 2020;197:108049. https://doi.org/10.1016/j.compositesb:2020.108049.
[33] Javanshour F, Ramakrishnan K, Layek RK, Laurikainen P, Prapavesis A, Kanerva M, et al. Effect of graphene oxide surface treatment on the interfacial adhesion and the tensile performance of flax epoxy composites. Compos Part A Appl Sci Manuf 2021:106270. https://doi.org/10.1016/j.compositesa.2020.106270.
[34] Fei P, Liao L, Cheng B, Song J. Quantitative analysis of cellulose acetate with a high degree of substitution by FTIR and its application. Anal Methods 2017;9:6194–201. https://doi.org/10.1039/c7ay02165h.
[35] Korkiakoski S, Sarlin E, Suihkonen R, Saarela O. Influence of reinforcement positioning on tension-tension fatigue performance of quasi-unidirectional GFRP laminates made of stitched fabrics. Compos Part B Eng 2017;112:38–48. https://doi.org/10.1016/j.compositesb.2016.12.017.
[36] Gamstedt EK, Sjögren BA. Micromechanisms in tension-compression fatigue of composite laminates containing transverse plies. Compos Sci Technol 1999;59(2):167–78. https://doi.org/10.1016/S0266-3538(98)00061-X.
[37] Yasaee M, Bond IP, Trask RS, Greenhalgh ES. Damage control using discrete thermoplastic film inserts. Compos Part A Appl Sci Manuf 2012;43(6):978–89. https://doi.org/10.1016/j.compositesa:2012.01.011.
[38] Xu Z, Yang F, Guan ZW, Cantwell WJ. An experimental and numerical study on scaling effects in the low velocity impact response of CFRP laminates. Compos Struct 2016;154:69–78. https://doi.org/10.1016/j.compstruct.2016.07.029.